



HAL
open science

**Pd Nanoparticles Supported on Ultrapure ZnO
Nanopowders as Reusable Multipurpose Catalysts**
Andrija Kokanović, Vladimir Ajdačić, Nataša Terzić Jovanović, Slavica
Stankic, Igor Opsenica

► **To cite this version:**

Andrija Kokanović, Vladimir Ajdačić, Nataša Terzić Jovanović, Slavica Stankic, Igor Opsenica. Pd Nanoparticles Supported on Ultrapure ZnO Nanopowders as Reusable Multipurpose Catalysts. ACS Applied Nano Materials, In press, 10.1021/acsanm.3c02743 . hal-04187430

HAL Id: hal-04187430

<https://hal.science/hal-04187430>

Submitted on 24 Aug 2023

HAL is a multi-disciplinary open access archive for the deposit and dissemination of scientific research documents, whether they are published or not. The documents may come from teaching and research institutions in France or abroad, or from public or private research centers.

L'archive ouverte pluridisciplinaire **HAL**, est destinée au dépôt et à la diffusion de documents scientifiques de niveau recherche, publiés ou non, émanant des établissements d'enseignement et de recherche français ou étrangers, des laboratoires publics ou privés.

Pd Nanoparticles Supported on Ultrapure ZnO Nanopowders as Reusable Multipurpose Catalysts

Andrija Kokanović^{a,c}, Vladimir Ajdačić^a, Nataša Terzić Jovanović^b, Slavica Stankić^{c}, Igor M. Opsenica^{d*}*

^a Innovative center, Faculty of Chemistry, Belgrade, Ltd., Studentski trg 16, 11158 Belgrade,
Serbia

^b University of Belgrade – Institute of Chemistry, Technology, and Metallurgy, National Institute
of the Republic of Serbia, Njegoševa 12, 11000 Belgrade, the Republic of Serbia

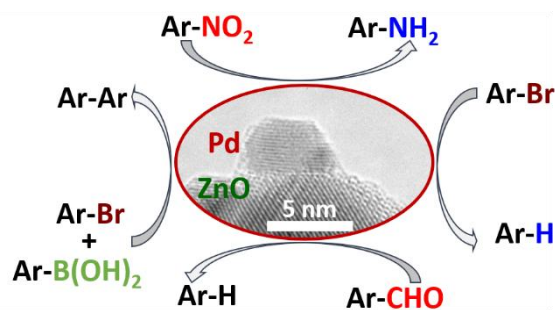
^c Sorbonne Université, CNRS UMR 7588, Institut des NanoSciences de Paris INSP, 4 place
Jussieu 75252 Paris cedex 05, France

^d University of Belgrade – Faculty of Chemistry, PO Box 51, Studentski trg 16, 11158 Belgrade,
Serbia

KEYWORDS: Palladium, Nanocatalyst, ZnO, Suzuki-Miyaura cross-coupling, nitroarenes, anilines, decarbonylation, hydrodebromination

ABSTRACT. Herein we report the synthesis and application of a highly active and versatile Pd/CVS-ZnO catalytic system. The two-step preparation of the catalyst includes chemical vapor synthesis (CVS) of ultrapure ZnO nanotetrapods, followed by liquid-phase in-situ reduction of a

Pd precursor and deposition of polycrystalline Pd nanoparticles (~6 nm). The as-synthesized catalyst was characterized using standard instrumental techniques. The catalyst was successfully applied in four chemical reactions: Suzuki-Miyaura cross-coupling, reduction of nitroarenes, decarbonylation and hydrodebromination of aromatic compounds, of which, the latter two are reported for the first time for Pd/ZnO catalytic system. The catalyst showed excellent activity within a wide range of substrates, delivering the products in high yields (70–99%). The recyclability of Pd/CVS-ZnO catalyst was tested within two different approaches. Firstly, the catalyst recyclability was examined in all four reactions, reusing the catalyst up to four times in Suzuki-Miyaura cross-coupling reaction, as well as reduction of 4-nitrobenzotrile, without significant loss of yield. Furthermore, the catalyst was successively used in three different reactions – showing a high degree of stability and delivering excellent product yields in all cases. In addition to its excellent activity, versatility and stability, the Pd/CVS-ZnO catalytic system also exhibited excellent recyclability over consecutive runs, which makes it a promising candidate for future application in complex industrial processes.



1. INTRODUCTION

The spotlight on catalysis and new catalyst development shines brighter each year. More than 90% of chemicals, such as fuels, fine chemicals, polymers and pharmaceuticals, rely intrinsically on catalytic processes for their production. Catalysts also play a role in sustainability and reducing the negative impact of industry on the environment. Therefore, there is a constant urge for obtaining versatile catalysts exhibiting high activity, which are readily available, stable under diverse reaction conditions and easily reusable.[1-4]

Pd-based catalysts are versatile and are employed extensively in academic as well as industrial synthetic processes. Homogenous Pd catalysts exhibit excellent activities owing to their well-defined and fully accessible active sites. However, inevitable product contamination and difficulties concerning catalyst recycling can make them unsuitable for use, especially in industries such as pharmaceutical.[5] Supported Pd nanoparticles (NPs) overcome these drawbacks as they can be readily separated from the product and reused.[6] Pd-catalyzed cross-coupling reactions are crucial carbon-carbon bond forming processes and are widely employed in academic as well industrial synthetic pathways.[7-10] Pd-catalyzed reduction reactions have extensive applicability, and are thus among the most studied in terms of Pd-based catalysis. For example, the reduction of nitroarenes provides valuable aniline-based precursors used for the production of various chemicals.[11-17] Furthermore, advances in heterogenous nitroarene reduction methods are important for environmental protection, as nitroarenes are ubiquitous water pollutants.[18] In addition to reduction reactions, many other useful Pd-catalyzed transformations, such as decarbonylation and dehalogenation of aromatic compounds, are applied in the synthesis of important compounds.[19]

ZnO NPs are cheap and simple to produce, non-toxic, environmental-friendly, and have good chemical and thermal stability, making them an attractive candidate for heterogeneous catalyst support.[20-22] Depending on the synthetic conditions, various shapes of ZnO NPs can be obtained.[23-26] ZnO NP tetrapods can be obtained via chemical vapor synthesis (CVS). Because CVS is conducted in the gas phase, it circumvents some drawbacks of liquid-based methods, such as the persistence of impurities, thereby ensuring high crystal purity.[27] ZnO tetrapods are rich in surface defects, such as oxygen vacancies, which have been shown to promote strong metal-support interactions.[27-29]

Pd supported on ZnO (Pd/ZnO) catalyst was utilized for the first time by Iwasa et al. for the methanol steam reforming process,[30,31] and it continues to be used for that purpose to date.[32-34] This catalytic system (Pd/ZnO) has also been applied in synthetic chemistry. Hosseini-Sarvari et al. synthesized the Pd/ZnO catalyst by the co-precipitation method. Pd and Zn nitrates, used as precursors, are dissolved in water and upon rising the reaction pH to 8, a precipitate is formed. After washing, drying and calcination, the catalyst was utilized in Suzuki-Miyaura and Hiyama reactions,[35,36] Mizoroki-Heck and Sonogashira reactions,[37] for the reduction of nitro-compounds,[38] and in C-O and C-N cross-coupling reactions.[36,39] Bao et al. prepared the Pd/ZnO catalyst by the hydrothermal route. Pd and Zn acetylacetonates were used as precursors, polyvinylpyrrolidone served as the stabilizing agent and *N,N*-dimethylformamide as the reduction agent. Precipitation and tuning of the ZnO morphology were done by adjusting the reaction pH with NaOH, acquiring different shaped Pd/ZnO catalysts. Their performance was compared in Suzuki-Miyaura cross-coupling reaction and reduction of 4-nitrophenol. All of the catalysts exhibited excellent activities in both reactions.[40] Hu et al. grew ZnO nanowires on Zn foil and placed them in an aqueous solution of Na₂PdCl₄, allowing the reduction and deposition

of Pd NPs to take place. The recyclability of Pd/ZnO nanowire arrays was tested in the Suzuki-Miyaura cross-coupling reaction and reduction of 4-nitrophenol, acquiring excellent results.[41]

In this study, we present a novel Pd/CVS-ZnO catalyst that exhibits excellent activity in several important and diverse chemical transformations. The ZnO support was synthesized via CVS method, which provide pure, highly crystalline ZnO nanopowder with tetrapod morphology (Figure 1). Pd NP deposition was accomplished via a more classical, solution-based method.[42] Catalyst characterization was achieved using TEM, HRTEM, SEM, XRD and ICP-QMS. Specific surface areas (S_{BET}) were determined from nitrogen sorption isotherms acquired at 77 K. The Pd/CVS-ZnO catalyst was tested in Suzuki-Miyaura cross-coupling reaction and reduction of nitroarenes (Figure 1), two reactions in which Pd/ZnO utilization was previously reported by the research groups mentioned above. In addition, the catalyst activity was examined in decarbonylation and hydrodebromination of aromatic compounds, which to the best of our knowledge has not yet been reported in the literature (Figure 1). Catalyst recyclability was also tested, and it was found that it can be reused up to four times, without significant loss of activity.

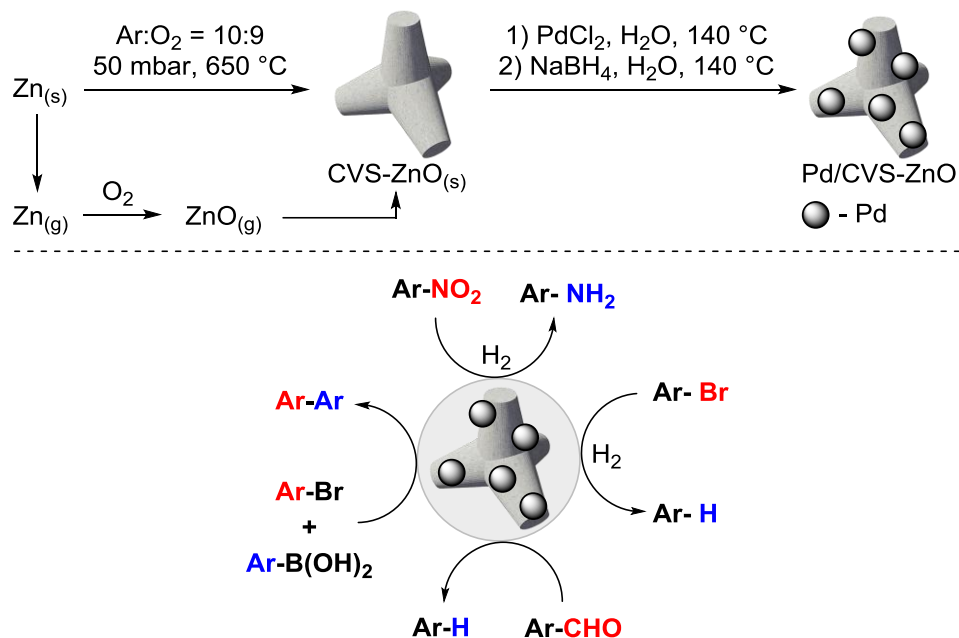


Figure 1. Synthesis and application of Pd/ CVS-ZnO catalyst.

2. EXPERIMENTAL SECTION

2.1. Chemicals and Materials. Zn pieces (>99.98%) were supplied by Goodfellow. PdCl₂ (≥99.9%) was supplied by Sigma Aldrich. NaBH₄ (≥99%) was supplied by Fluka. All chemicals and solvents were supplied by Sigma-Aldrich, if not stated otherwise. All chemicals were directly used without further purification.

2.2. Preparation of CVS-ZnO Support.

As starting material, high purity Zn pieces (>99.98%) was used. Zn pieces were placed in a gas flow reactor and the reactor was evacuated using a primary pump. The Ar and O₂ flows were set at 1000 sccm and 900 sccm, respectively. The evaporation temperature of metallic Zn was chosen to correspond to a Zn vapor pressure of 1 mm Hg (1.33 mbar). Formed in the gas-phase at elevated temperature, CVS ZnO nanoparticles are finally collected on the stainless-steel net at room temperature and in form of powder.

2.3. Synthesis of Pd/CVS-ZnO Catalyst.

Pd-deposition on as-prepared CVS-ZnO powder was carried out in line with previously reported procedure.[42] A cuvette containing a suspension of CVS-ZnO (450 mg) in degassed H₂O (7 mL) was purged with argon. Upon adding PdCl₂ (56 mg, 0.32 mmol) the cuvette was sealed and heated at 140 °C for 0.5 h. Then, the reaction mixture was cooled to room temperature and a solution of NaBH₄ (380 mg, 10.02 mmol) in degassed H₂O (3 mL) was added dropwise, under argon atmosphere. The reaction mixture was stirred at room temperature until the production of hydrogen stopped. Afterwards, the cuvette was sealed again and the reaction mixture was stirred (1000 rpm) and heated at 140 °C. After 24 h the solid product was centrifuged and washed several times with deionized H₂O. The catalyst was dried under vacuum at 65 °C for 2 h, to obtain Pd/CVS-ZnO (466 mg).

2.4. General procedure for Suzuki-Miyaura cross-coupling reaction.

To a round-bottom reaction flask purged with argon and equipped with a magnetic stir bar and a reflux condenser, **1a** (30.3 mg, 0.15 mmol), **2a** (20.1 mg, 0.165 mmol), Pd/CVS-ZnO (4.6 mg, 1 mol% Pd), Na₂CO₃ (60.4 mg, 0.57 mmol), H₂O (0.5 mL) and DMF (0,5 mL) were added. The reaction mixture was purged with argon and heated at 65 °C for 5 h. The reaction mixture was filtered through a thin layer of silica gel and the layer was washed with *n*-hexane (5 × 2 mL). The organic layer was separated and washed with brine (1 × 5 ml) and the solvent was removed under reduced pressure, to afford **3a** (29.9 mg, 99%) as a pale yellow solid.

2.5. General procedure for the reduction of nitroarenes.

To a round-bottom reaction flask equipped with a magnetic stir bar, **3a** (29.9 mg, 0,15 mmol), Pd/CVS-ZnO (4.6 mg, 1 mol% Pd) and MeOH (2.0 mL) were added and hydrogen was introduced to the reaction mixture with a balloon for 4 h at room temperature. The reaction

mixture was filtered through a thin layer of silica gel and the layer was washed with CH₂Cl₂ (5 × 2 mL). The solvent was removed under reduced pressure to afford **5a** (25.4 mg, 99%) as a yellow solid.

2.6. General procedure for the hydrodebromination of bromoarenes.

To a round-bottom reaction flask equipped with a magnetic stir bar, **6a** (31.1 mg, 0.15 mmol), Pd/CVS-ZnO (4.6 mg, 1 mol% Pd) and MeOH (2.0 mL) were added and hydrogen was introduced to the reaction mixture with a balloon for 4 h at room temperature. The reaction mixture was filtered through a thin layer of silica gel and the layer was washed with CH₂Cl₂ (5 × 2 mL). The solvent was removed under reduced pressure to afford the product **7a** (19.2 mg, 99%) as a white solid.

2.7. General procedure for the decarbonylation of aromatic aldehydes.

To a dry glass reaction tube purged with argon and equipped with a magnetic stir bar, **8a** (27.3 mg, 0.15 mmol), Pd/CVS-ZnO (13.7 mg, 3 mol% Pd) and cyclohexane (1.0 mL) were added and the sealed tube was heated at 140 °C for 24 h. The reaction mixture was filtered through a thin layer of silica gel and the layer was washed with CH₂Cl₂ (5 × 2 mL). The solvent was removed under reduced pressure to obtain the product **9a** (23,1 mg, 99%) as a white solid.

3. RESULTS AND DISCUSSION

3.1. Synthesis of Pd/CVS-ZnO Catalyst.

Pd/CVS-ZnO was prepared via a two-step synthetic process. Firstly, ZnO nanopowder was obtained by vapor-phase-based method, namely chemical vapor synthesis (CVS). Low pressure and high temperature allow metallic Zn atoms to transfer to gas phase, and the gas flow reactor ensures that the combustion takes place in a controlled Ar/O₂ ratio. Such constant purging

guaranties conditions in which ultrapure ZnO nanotetrapod powder is obtained. Given the low total pressure during the CVS process (50 mbar) – provided by primary vacuum pumping – the synthesis conditions are considered as oxygen deficient.[27] To preserve from any external contaminations, ZnO powders were maintained either under dynamic vacuum conditions ($P < 10^{-5}$ mbar) or supersaturated Ar-atmosphere during the storage, transport and handling. The specific surface area was measured to be $S_{\text{BET}} = 29.4 \pm 1.0 \text{ m}^2/\text{g}$.

The synthesis condition controlled within the CVS-flow reactor provide a strongly non-stoichiometric ZnO – as reflected in a bright yellowish color of this powder. The absorption of visible light and the resulting coloration has recently been established to result from point defects present in the oxide's crystal structure.[27] In line with the conditions afforded during the crystal formation, oxygen vacancies were identified to be the main defects in this type of ZnO, both on the surface and in the bulk. Point defects, in particular neutral oxygen vacancies (electron rich) provide conditions to serve not only as exceptional nucleation sites but may also boost the metal-support interaction affecting in final both, the catalyst stability and its overall activity.[43,44]

In the second step, the Pd-deposition on as-prepared CVS-ZnO powder was carried out in line with previously reported procedure.[42] Upon addition of the reducing agent to an aqueous suspension of the Pd precursor and CVS-ZnO, a black precipitate was formed. The suspension was left overnight, under constant heating and vigorous stirring, to allow the deposition of Pd NPs to take place. Afterwards, the formed Pd/CVS-ZnO catalyst was washed, dried and kept either under dynamic vacuum conditions ($P < 10^{-5}$ mbar) or supersaturated Ar-atmosphere during the storage, transport and handling. ICP-QMS analysis showed an amount of 3.5 wt% Pd to be deposited on CVS-ZnO powder. The specific surface area was measured to be $S_{\text{BET}} = 41.6 \pm 2.5 \text{ m}^2/\text{g}$. Provided that very small Pd particles were deposited (mean size ~6nm), the addition

of a new phase at the surface of ZnO substrate creates additional heterogeneity and roughness which results in a higher surface area. Moreover, during the liquid phase deposition of palladium the ZnO nanopowder is exposed to rather aggressive conditions. Likely this may provoke the etching of its surface and cause it to roughen that would also lead to an enhanced specific surface area.

3.2. Characterization of Pd/CVS-ZnO Catalyst.

The morphologies of CVS-ZnO and Pd/CVS-ZnO were characterized by SEM and TEM microscopies. The representative SEM and TEM images of CVS-ZnO powder (observed to be yellowish in color) are shown in Figure 2b and Figure 2c, respectively. As seen from SEM image CVS-ZnO exhibits a strong degree of agglomeration with tetrapod-like structures of irregular sizes. Closer inspection by TEM (Figure 2c) confirms that the as-prepared nanoparticles of CVS-ZnO are typically tetrapod-like structures with four needle-like arms that originate from the center of the polyhedron. The length of the tetrapods arms has been observed not to exceed 60 nm while the corresponding diameter scale to lower than 30 nm. Such morphology is typical of ZnO produced by combustion techniques and implies the presence of non-polar facets (10-10), (11-20) to be strongly favored over the two polar faces (0001) and (000-1).[45]

TEM and HRTEM images representative of the Pd/CVS-ZnO catalyst are shown in Figure 2d and 2e, respectively. Comparing TEM shown in Figure 2c and Figure 2d, a significant morphological change can be observed to occur on ZnO upon Pd-loading. An average size of ~6 nm was estimated for Pd nanoparticles by electron microscopy (see the Supporting Information, Figure S1). In HRTEM (Figure 2e), polycrystalline domains can be observed along with a family of planes with distances of 0.224 nm. This d-spacing corresponds to Pd(111) planes and was

previously reported in multiple studies.[46] Interestingly, the shape of Pd nanoparticles shown in HRTEM in Figure 2e resembles to a truncated octahedron, the close-to equilibrium shape that is typically observed for supported metallic nanoparticles obtained by co-combustion synthesis.[47]

X-ray diffraction patterns acquired on CVS-ZnO (green curve) and Pd/ CVS-ZnO (red curve) powders are compared in Figure 2a. Sharp and narrow diffraction peaks can be observed in both diffractograms indicating a high crystal quality of powders. According to the X-ray profile analysis, CVS-ZnO exhibits hexagonal, wurtzite structure. No extra diffraction peaks were detected indicating that this ZnO is purely monophasic with crystals free of any impurities. The lattice parameters are calculated by the Rietveld refinement analysis, to be $a = b = 3.250 \text{ \AA}$, $c = 5.207 \text{ \AA}$. These values are consistent with the lattice parameters reported in literature and database.[48] Upon Pd-loading (red curve), the ZnO-phase remains highly preserved with one additional diffraction peak detected at 40.3° (indicated by star in red curve) in XRD spectrum of Pd/ CVS-ZnO. The value of 2θ matches with the diffraction of (111) planes in metallic Pd which is in agreement with crystallographic database.[49] Upon closer examination, two additional Pd signals can be observed – a low intensity peak representing the (200) lattice at 46.6° , and a peak at 68.0° , included in the ZnO peak found at 67.9° , which corresponds to the (220) lattice. Low intensity of Pd peaks is in line with the low quantity of Pd loaded on CVS-ZnO surface as well as with the small size of Pd particles observed in TEM. On the other hand, the relatively large width of this peak indicates a polycrystalline phase of Pd particles – as also seen in HRTEM images.

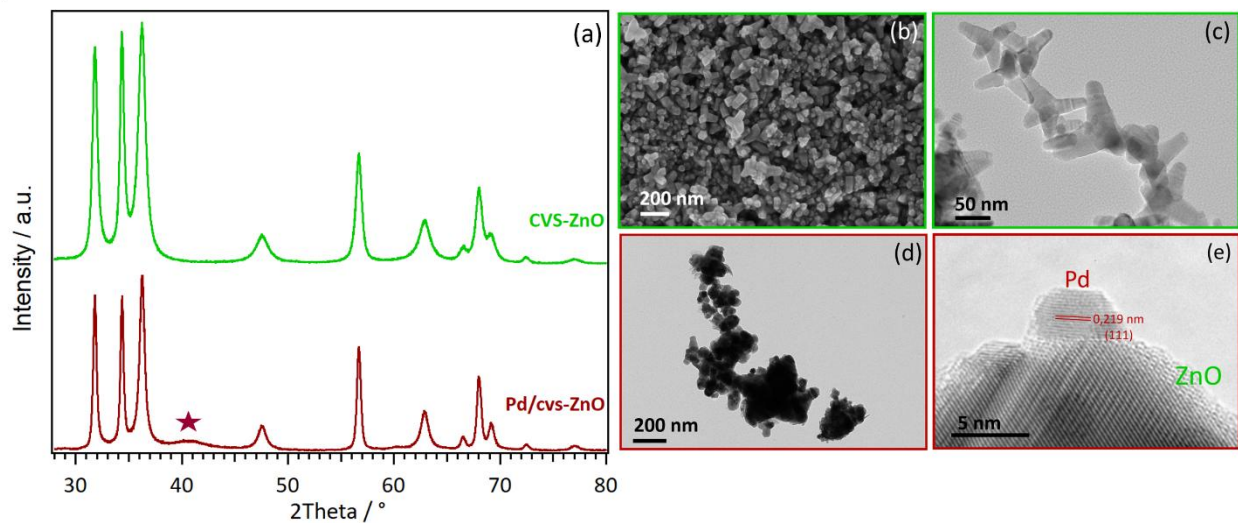
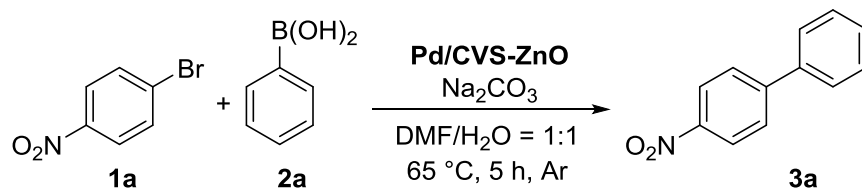


Figure 2. (a) XRD patterns, (b,c) SEM and TEM images of CVS-ZnO nanopowders, (d,f) TEM and HRTEM images of Pd/ CVS-ZnO nanopowders. Diffraction peak typical of Pd (111) is indicated by star in red curve.

3.3. Catalytic Performances of Pd/ CVS-ZnO Catalyst.

Initially, we examined the catalytic activity of the Pd/ CVS-ZnO catalyst in the Suzuki-Miyaura cross-coupling reaction. The coupling between 4-bromonitrobenzene and phenylboronic acid was chosen as the model reaction. The effects of catalyst loading in the Suzuki-Miyaura reaction were initially investigated using a water/DMF solvent system at a temperature of 65 °C. In the presence of 3 mol% of Pd and Na₂CO₃ as the base, the desired product **3a** was isolated in excellent yield (Table 1, entry 1). Decreasing the amount of Pd from 3 mol% to 1 mol% did not lead to changes in the yield (Table 1, entry 2). However, further decreases to 0.5 mol% and 0.1 mol% of Pd resulted in only trace amounts of the desired product being isolated. (Table 1, entries 3-4). Notably, when Suzuki-Miyaura reaction was performed in EtOH/H₂O solvent system, the desired product was not detected.

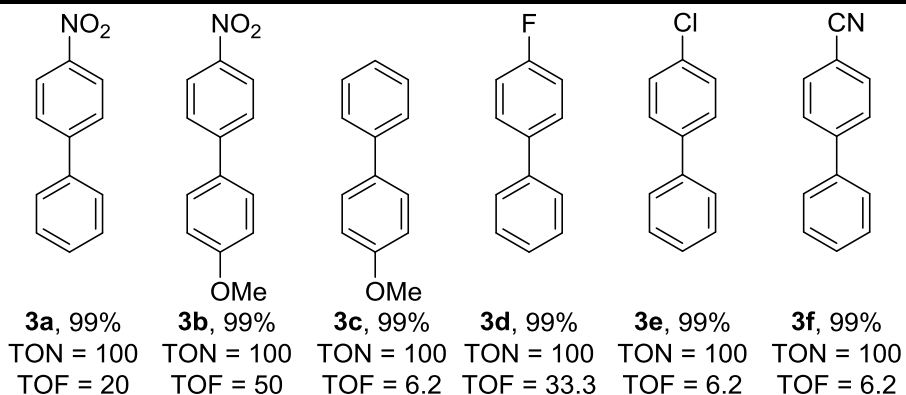
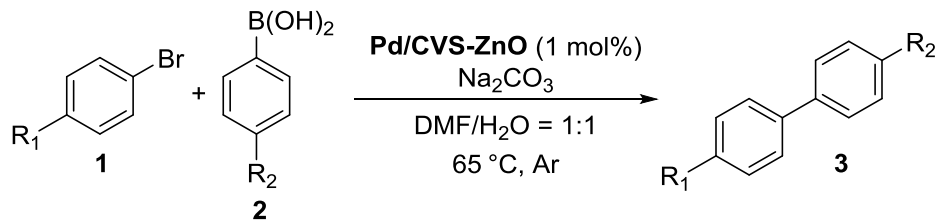
Table 1. Optimization of the reaction conditions for Suzuki-Miyaura coupling^a

entry	Catalyst (mol%)	Yield (%) ^b
1	Pd/CVS-ZnO (3 mol%)	99
2	Pd/CVS-ZnO (1 mol%)	99
3	Pd/CVS-ZnO (0.5 mol%)	trace
4	Pd/CVS-ZnO (0.1 mol%)	trace

^a) Reaction conditions: **1a** (0.15 mmol), **2a** (0.165 mmol), Na₂CO₃ (0.57 mmol), DMF (0.5 mL), H₂O (0.5 mL), 65 °C, argon ^b) Isolated yield.

With the optimal conditions in hand, the substrate scope of the reaction was explored using various aryl bromides **1** and boronic acids **2**. Gratifyingly, various biaryl compounds bearing an electron-rich group, such as methoxy, or electron-withdrawing groups such as nitro, cyano, chloro and fluoro, were produced in excellent yields (99%) (Table 2, **3a-3f**). Notably, the products were isolated in sufficient purity following extraction, without the need for chromatography. The catalytic activity of Pd/CVS-ZnO in the Suzuki-Miyaura cross-coupling reaction is comparable with the activity of the previously reported Pd/ZnO catalysts (see the Supporting Information, Table S1).[35,36,40,41]

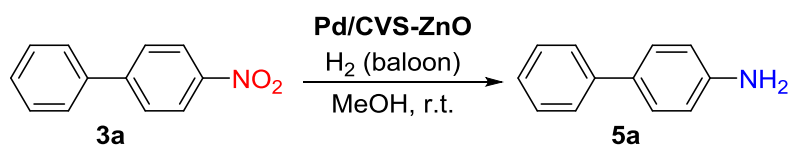
Table 2. Substrate scope of the Suzuki-Miyaura coupling reaction^a



^{a)} Reaction conditions: **1a** (0.15 mmol), **2a** (0.165 mmol), Na₂CO₃ (0.57 mmol), DMF (0.5 mL), H₂O (0.5 mL), argon.

The catalytic activity of Pd/CVS-ZnO was further explored for the reduction of nitroarenes. Compound **3a**, obtained previously via Suzuki-Miyaura cross-coupling, was used as a model substrate. The reduction of **3a** was first examined using Pd/CVS-ZnO (3 mol % of Pd), H₂ (1 atm.) in MeOH at room temperature. The reaction was complete within 4 h, and the desired product **5a** was isolated in an excellent yield (99%). (Table 3, entry 1). A decrease in the catalyst amount to 1 mol% of Pd did not impact the reaction efficiency negatively (Table 3, entry 2). Meanwhile, when the amount of the catalyst was decreased from 1 mol% to 0.5 mol%, the efficiency deteriorated, and product **5a** was obtained in lower yield (Table 3, entry 3). Prolonging the reaction time did not increase the yield of the desired product **5a** significantly (Table 3, entry 4).

Table 3. Optimization of reaction conditions for the reduction of nitroarenes^a

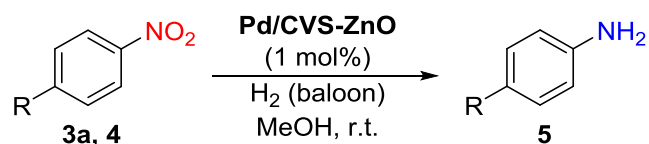


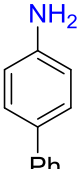
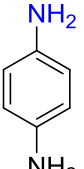
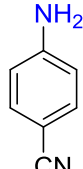
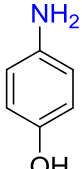
entry	Catalyst (mol%)	time (h)	Yield (%) ^b
1	Pd/CVS-ZnO (3 mol%)	4	99
2	Pd/CVS-ZnO (1 mol%)	4	99
3	Pd/CVS-ZnO (0.5 mol%)	4	27
4	Pd/CVS-ZnO (0.5 mol%)	24	43

^aReaction conditions: (0,15 mmol), H₂ (balloon), ^bIsolated yield.

The reduction of nitroarenes bearing electron donating groups (-Ph, -NH₂, -OH) and an electron withdrawing group (-CN) at the *para*-position was performed under the optimized conditions. The corresponding anilines were obtained in excellent yields (Table 4, **5a-5d**). The catalytic activity of Pd/CVS-ZnO in the reduction of nitroarenes is comparable with the activity of the previously reported Pd/ZnO catalysts (see the Supporting Information, Table S2).[38,40]

Table 4. Substrate scope of nitroarene reduction^a

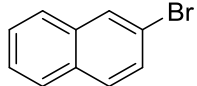
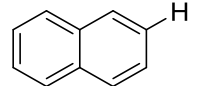


			
5a , 99% ^b	5b , 99% ^b	5c , 99% ^b	5d , 99% ^b
TON = 100	TON = 100	TON = 100	TON = 100
TOF = 25	TOF = 33.3	TOF = 33.3	TOF = 4.2

^a)Reaction conditions: (0,15 mmol), H₂ (balloon), MeOH (1 mL). ^b)Isolated yield.

Additionally, we examined the activity of the catalyst for the hydrodebromination of aryl bromides. The reaction conditions were optimized using 2-bromonaphthalene (**6a**) as the model substrate. It was found that the same reaction conditions used for the reduction of nitroarenes can be used in the hydrodebromination reaction (Table 5, entry 3). Notably, when the reaction was performed in the absence of H₂ the desired product was not formed.

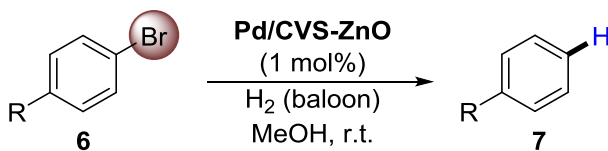
Table 5. Optimization of reaction conditions for the hydrodebromination of bromoarenes^a

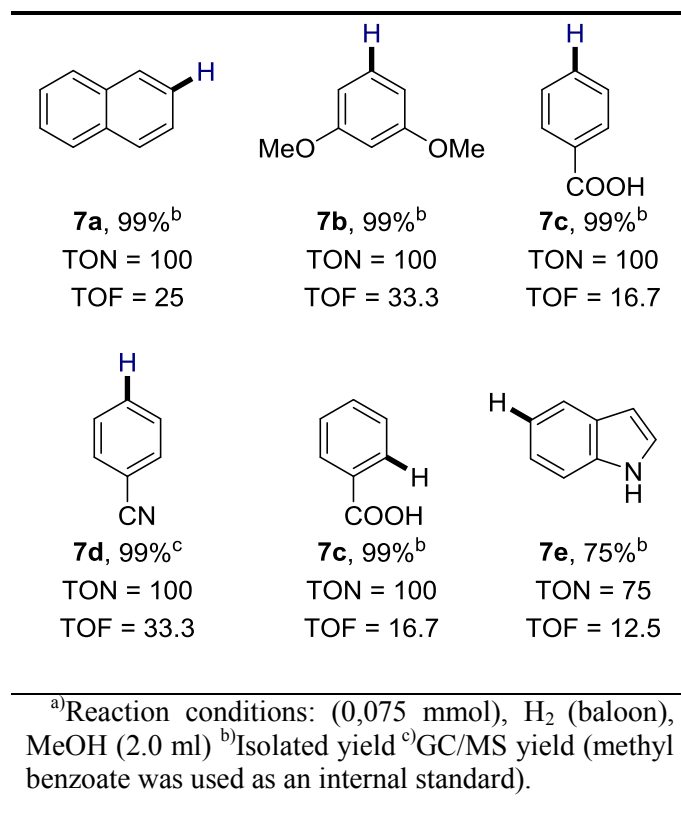
	Pd/CVS-ZnO H ₂ (balloon) MeOH, r.t., 4 h	
6a		7a
entry	Catalyst (mol%)	Yield (%) ^b
1	Pd/CVS-ZnO (5 mol%)	99
2	Pd/CVS-ZnO (3 mol%)	99
3	Pd/CVS-ZnO (1 mol%)	99

^a)Reaction conditions: (0,075 mmol), H₂ (balloon), MeOH (2.0 mL), ^b)Isolated yield.

With the optimized reaction conditions in hand (Table 5, entry 3), the substrate scope for the hydrodebromination of bromoarenes catalyzed by Pd/CVS-ZnO was investigated. Bromoarenes bearing *m,m*-OMe, *p*-COOH and *p*-CN substituents were converted to the corresponding dehalogenated products **7b–7d** in near quantitative yields (Table 6). These results showed that the electronic effects of the substituents on bromobenzene did not have an impact on the reaction efficiency. In addition, the sterically hindered 2-bromobenzoic acid was successfully converted into benzoic acid **7c** (Table 6). Furthermore, indole **7e** was obtained in good yield after hydrodebromination of 5-bromoindole (Table 6).

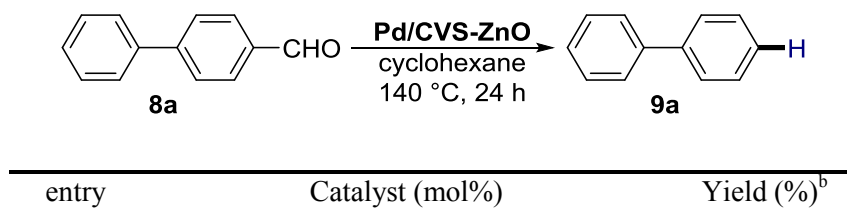
Table 6. Substrate scope of the hydrodebromination reaction^a





Finally, we used the Pd/CVS-ZnO catalytic system in the decarbonylation reaction. Relying on our previous experience, we chose cyclohexane as the optimal solvent for this reaction.[50] After optimizing the reaction conditions, the protocol consisting of Pd/CVS-ZnO (3 mol %) in cyclohexane at 140 °C under argon atmosphere gave the best results. The desired biphenyl **9a** was isolated in an excellent yield (Table 7).

Table 7. Optimization of reaction conditions for the decarbonylation of aldehydes^a

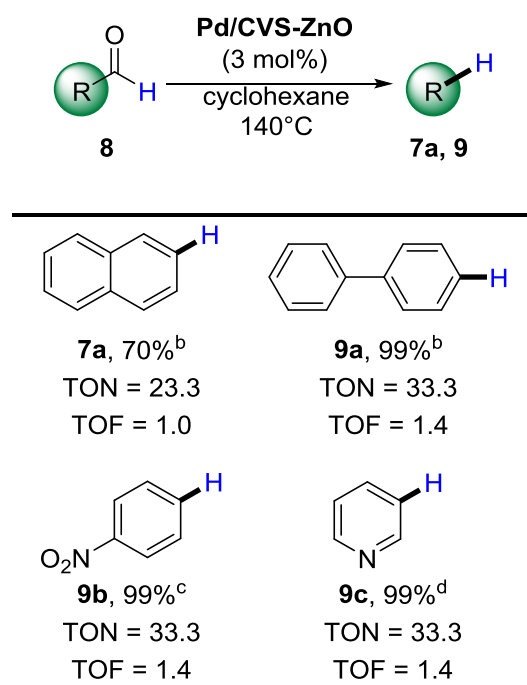


1	Pd/CVS-ZnO (5 mol%)	99
2	Pd/CVS-ZnO (3 mol%)	99
3	Pd/CVS-ZnO (1 mol%)	11

^{a)} Reaction conditions: (0.165 mmol), cyclohexane (2.0 mL), argon
^{b)} Isolated yield

Having established the optimized reaction conditions, we explored the scope of various aromatic and heteroaromatic aldehydes (Table 8). When 2-naphthaldehyde (**8a**) was used as the substrate, the decarbonylated product **7a** was isolated in a good yield. Decarbonylation of *p*-nitrobenzaldehyde under optimized conditions provided the desired product **9b** in excellent yield. Moreover, 3-pyridinecarboxaldehyde, a more challenging heterocyclic aldehyde, was converted to the decarbonylated product **9c** in near quantitative yield.

Table 8. Substrate scope of the decarbonylation reaction^a



^aReaction conditions: (0,165 mmol), cyclohexane (2.0 mL), 24h ^bIsolated yield ^cGC/MS yield methyl benzoate was used as an internal standards). ^dGC/MS yield naphthalene was used as an internal standards).

Recyclability of the Pd/CVS-ZnO catalyst was tested in all four reactions: the synthesis of **3d** via Suzuki-Miyaura cross-coupling reaction, reduction of 4-nitrobenzonitrile, hydrodebromination of 2-bromonaphthalene and decarbonylation of [1,1'-biphenyl]-4-carbaldehyde (Figure 3). For the Suzuki-Miyaura cross-coupling reaction and catalytic reduction of 4-nitrobenzonitrile nearly quantitative yields of the reaction products were obtained after four catalytic cycles, with a slight decrease in yield after the fifth cycle. This decrease may be attributed to small amounts of Pd leaching from the catalyst, as detected by ICP-QMS. The analysis shows 0,98 ppm of Pd leaching after the first catalytic cycle. It was found that the mechanism of Pd nanoparticles catalyzed C–C coupling reactions can be homogeneous, heterogeneous, or a mixture of those two mechanisms (oxidative addition at Pd NP surface followed by leaching of the [Pd(Ar)X] species which goes through the homogeneous catalytic cycle).[51-54] The loss of catalytic activity in the recyclability test of Suzuki-Miyaura cross-coupling reaction could be the result of homogeneous or mixed (homogeneous-heterogeneous) reaction mechanism. Thus, result of recyclability test implies that redeposition of homogeneous palladium species on to the CVS-ZnO support is not efficient enough. Finally, for the catalytic hydrodebromination of 2-bromonaphthalene and decarbonylation of [1,1'-biphenyl]-4-

carbaldehyde nearly quantitative yields of the reaction product were obtained after three and two catalytic cycles, respectively.

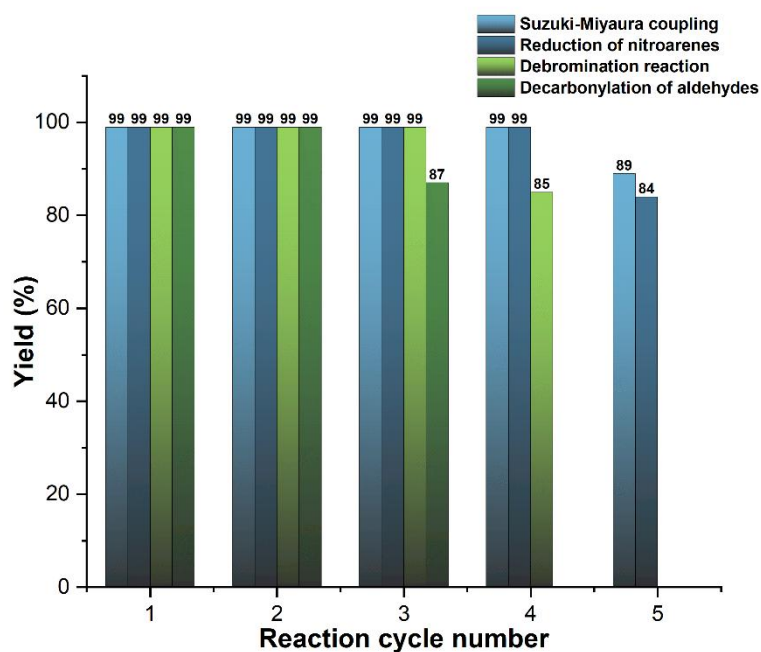
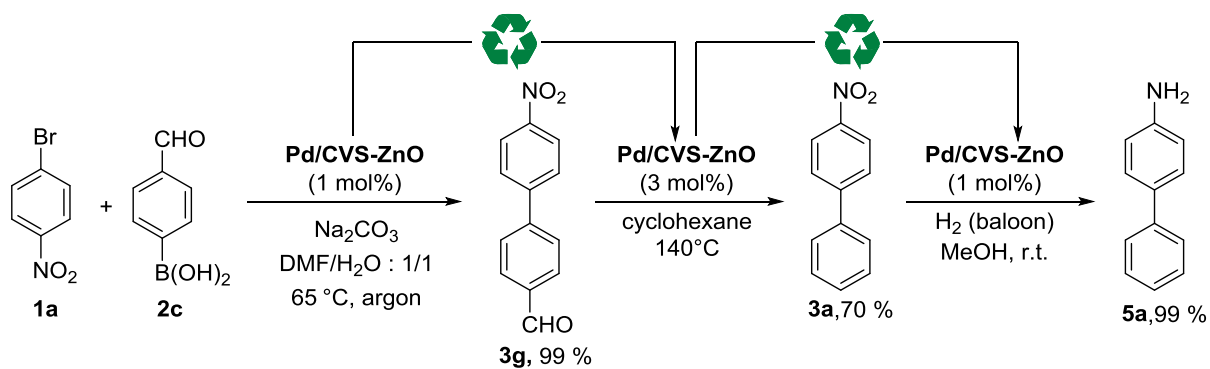


Figure 3. Recyclability of Pd/CVS-ZnO catalyst.

Finally, as a proof of concept, compound **5a** was synthesized in three reaction steps, using the same batch of Pd/CVS-ZnO catalyst in each transformation (Scheme 1).



Scheme 1. Proof of concept.

4. CONCLUSION

In summary, the Pd/CVS-ZnO catalyst was obtained in a two-step process: chemical vapor synthesis of the ZnO support followed by the deposition of Pd in a liquid phase. The presence of Pd was confirmed by using X-ray diffraction and ICP-QMS while the electron microscopy observations indicated ~6 nm-sized Pd distributed over tetrapod-like ZnO particles. The catalyst exhibited high catalytic activity in four diverse chemical transformations, including: Suzuki-Miyaura cross-coupling, reduction of nitroarenes, decarbonylation and hydrodebromination of aromatic compounds. The turnover numbers (TONs) for Suzuki-Miyaura cross-coupling, reduction of nitroarenes and hydrodebromination of aromatic compounds are 100, with exception of **7e** obtained in the hydrodebromination of 5-bromoindole. The TONs for decarbonylation are lower (TONs = 23.3-33.3) since more catalyst was required for the successful transformation. The turnover frequency (TOF) were calculated for all Pd/CVS-ZnO catalyzed reactions, ranging from 1.0 to 50, as a result of prolonged reaction time. Notably, the catalyst was applied to three different reactions in a consecutive manner, withstanding various reaction conditions and providing desired products in high yields. Leaching analysis indicated <1 ppm concentration of residual Pd, suggesting the suitability of this catalytic system for the application in industries,

such as pharmaceutical, which do not tolerate high concentrations of heavy metals in products (no more than 10 ppm). The high activity and stability in diverse chemical reactions, amenability to recycling and re-use in further transformations of the Pd/CVS-ZnO catalyst, make it an adequate candidate for further examination and potential industrial application.

ASSOCIATED CONTENT

Supporting Information.

The Supporting Information is available free of charge at <https://pubs.acs.org/doi/10.1021/>

Copies of ¹H and ¹³C NMR spectra for the synthesized compounds (PDF)

AUTHOR INFORMATION

Corresponding Authors:

Slavica Stankic – Sorbonne Université, CNRS UMR 7588, Institut des NanoSciences de Paris
INSP, 4 place Jussieu 75252 Paris cedex 05, France

ORCID: 0000-0002-8711-9746

E-mail: slavica.stankic@insp.jussieu.fr

Igor M. Opsenica – University of Belgrade – Faculty of Chemistry, PO Box 51, Studentski trg
16, 11158 Belgrade, Serbia

ORCID: 0000-0003-4942-4042

E-mail: igorop@chem.bg.ac.rs

Author Contributions

The manuscript was written through contributions of all authors. All authors have given approval to the final version of the manuscript.

Notes

The authors declare no competing financial interest.

ACKNOWLEDGMENT

Financial support from the Ministry of Science, Technological Development and Innovation of Republic of Serbia Contract numbers: 451-03-47/2023-01/200168, 451-03-47/2023-01/200288. The authors are grateful to Ferdaous Ben Romdhane from Fédération de Chimie et Matériaux de Paris-Centre FCMat, Sorbonne Université, for the TEM data collection and interpretation, Jean-Eudes Duvauchelle and Isabelle Trimaille, from Institut des NanoSciences de Paris, Sorbonne Université, (INSP) for the XRD and SBET measurements, respectively.

ABBREVIATIONS

Pd/CVS-ZnO, Pd-supported CVS-ZnO Nanopowders

CVS, chemical vapor synthesis

NPs, nanoparticles

TEM, transmission electron microscopy

HRTEM, high-resolution transmission electron microscopy

SEM, scanning electron microscopy

XRD, X-ray diffraction

ICP-QMS, quadrupole inductively coupled plasma mass spectrometry

S_{BET}, specific surface areas

REFERENCES

- (1) Cui, X.; Li, W.; Ryabchuk, P.; Junge, K.; Beller, M. Bridging homogeneous and heterogeneous catalysis by heterogeneous single-metal-site catalysts. *Nat. Catal.* **2018**, *1*, 385–397.
- (2) Fechete, I.; Wang, Y.; Védrine, J. C. The past, present and future of heterogeneous catalysis. *Catal. Today* **2012**, *189*, 2–27.
- (3) Li, Z.; Ji, S.; Liu, Y.; Cao, X.; Tian, S.; Chen, Y.; Niu, Z.; Li, Y. Well-Defined Materials for Heterogeneous Catalysis: From Nanoparticles to Isolated Single-Atom Sites. *Chem. Rev.* **2020**, *120*, 623–682.
- (4) Chen, B. W. J.; Xu, L.; Mavrikakis, M. Computational Methods in Heterogeneous Catalysis. *Chem. Rev.* **2021**, *121*, 1007–1048.
- (5) Tao, R.; Ma, X.; Wei, X.; Jin, Y.; Qiu, L.; Zhang, W. Porous organic polymer material supported palladium nanoparticles. *J. Mater. Chem. A* **2020**, *8*, 17360–17391.
- (6) Blaser, H.-U.; Indolese, A.; Schnyder, A.; Steiner, H.; Studer, M. Supported palladium catalysts for fine chemicals synthesis. *J. Mol. Catal. A: Chem.* **2001**, *173*, 3–18.

- (7) Das, M. K.; Bobb, J. A.; Ibrahim, A. A.; Lin, A.; AbouZeid, K. M.; El-Shall, M. S. Green Synthesis of Oxide-Supported Pd Nanocatalysts by Laser Methods for Room-Temperature Carbon-Carbon Cross-Coupling Reactions. *ACS Appl. Mater. Interfaces* **2020**, *12*, 23844–23852.
- (8) Choe, H. R.; Han, S. S.; Kim, Y.-I.; Hong, C.; Cho, E. J.; Nam, K. M. Understanding and Improving Photocatalytic Activity of Pd-Loaded BiVO₄ Microspheres: Application to Visible Light-Induced Suzuki-Miyaura Coupling Reaction. *ACS Appl. Mater. Interfaces* **2021**, *13*, 1714–1722.
- (9) Phan, N. T. S.; Van Der Sluys, M.; Jones, C. W. On the Nature of the Active Species in Palladium Catalyzed Mizoroki-Heck and Suzuki-Miyaura Couplings – Homogeneous or Heterogeneous Catalysis, A Critical Review. *Adv. Synth. Catal.* **2006**, *348*, 609–679.
- (10) Pagliaro, M.; Pandarus, V.; Ciriminna, R.; Béland, F.; Carà, P. D. Heterogeneous versus Homogeneous Palladium Catalysts for Cross-Coupling Reactions. *ChemCatChem* **2012**, *4*, 432–445.
- (11) Kadam, H. K.; Tilve, S. G. Advancement in methodologies for reduction of nitroarenes. *RSC Adv.* **2015**, *5*, 83391–83407.
- (12) Wen, L.; Wang, D.; Xi, J.; Tian, F.; Liu, P.; Bai, Z.-W. Heterometal modified Fe₃O₄ hollow nanospheres as efficient catalysts for organic transformations. *J. Catal.* **2022**, *413*, 779–785.

(13) Wang, D.; Li, Y.; Wen, L.; Xi, J.; Liu, P.; Hansen, T. H.; Li, P. Ni-Pd-Incorporated Fe₃O₄ Yolk-Shelled Nanospheres as Efficient Magnetically Recyclable Catalysts for Reduction of N-Containing Unsaturated Compounds. *Catalysts*, **2023**, *13*, 190.

(14) Zhang, N.; Qiu, Y.; Sun, H.; Hao, J.; Chen, J.; Xi, J.; Liu, J.; He, B.; Bai, Z.-W. Substrate-Assisted Encapsulation of Pd-Fe Bimetal Nanoparticles on Functionalized Silica Nanotubes for Catalytic Hydrogenation of Nitroarenes and Azo Dyes. *ACS Appl. Nano Mater.* **2021**, *4*, 5854–5863.

(15) Xi, J.; Huang, J.; Wang, D.; Wen, L.; Hao, J.; He, B.; Chen, J.; Bai, Z.-W. Probing Activity Enhancement of Photothermal Catalyst under Near-Infrared Irradiation. *J. Phys. Chem. Lett.* **2021**, *12*, 3443–3448.

(16) Xi, J.; Sun, H.; Wang, D.; Zhang, Z.; Duan, X.; Xiao, J.; Xiao, F.; Liu, L.; Wang, S. Confined-interface-directed synthesis of Palladium single-atom catalysts on graphene/amorphous carbon. *Appl. Catal., B* **2018**, *225*, 291–297.

(17) Huang, J.; Li, X.; Xie, R.-H.; Tan, X.; Xi, J.; Tian, F.; Liu, P.; Hansen, T. W.; Bai, Z.-W. Defect anchoring of atomically dispersed Pd on nitrogen-doped holey carbon nanotube for catalytic hydrogenation of nitroarenes. *Appl. Surf. Sci.* **2023**, *615*, 156344.

(18) Çalışkan, M.; Akay, S.; Kayan, B.; Baran, T. Fabrication of palladium nanocatalyst supported on magnetic eggshell and its catalytic character in the catalytic reduction of nitroarenes in water. *J. Organomet. Chem.* **2021**, *950*, 121978.

- (19) Ajdačić, V.; Nikolić, A.; Simić, S.; Manojlović, D.; Stojanović, Z.; Nikodinovic–Runic, J.; Opsenica, I. M. Decarbonylation of Aromatic Aldehydes and Dehalogenation of Aryl Halides Using Maghemite–Supported Palladium Catalyst. *Synthesis* **2018**, *50*, 119–126.
- (20) Sun, Y.; Chen, L.; Bao, Y.; Zhang, Y.; Wang, J.; Fu, M.; Wu, J.; Ye, D. The Applications of Morphology Controlled ZnO in Catalysis. *Catalysts* **2016**, *6*, 188.
- (21) Wang, Z. L. Zinc oxide nanostructures: growth, properties and applications. *J. Phys.: Condens. Matter* **2004**, *16*, 829–858.
- (22) Kołodziejczak-Radzimska, A.; Jesionowski, T. Zinc Oxide–From Synthesis to Application: A Review. *Materials* **2014**, *7*, 2833–2881.
- (23) Xu, L.; Hu, Y.–L.; Pelligra, C.; Chen, C.–H.; Jin, L.; Huang, H.; Sithambaram, S.; Aindow, M.; Joesten, R.; Suib, S. L. ZnO with Different Morphologies Synthesized by Solvothermal Methods for Enhanced Photocatalytic Activity. *Chem. Mater.* **2009**, *21*, 2875–2885.
- (24) Shouli, B.; Liangyuan, C.; Dainqing, L.; Wensheng, Y.; Pengcheng, Y.; Zhiyong, L.; Aifan, C.; Liu, C. C. Different morphologies of ZnO nanorods and their sensing property. *Sens. Actuators B* **2010**, *146*, 129–137.
- (25) Tong, Y.; Liu, Y.; Dong, L.; Zhao, D.; Zhang, J.; Lu, Y.; Shen, D.; Fan, X. Growth of ZnO Nanostructures with Different Morphologies by Using Hydrothermal Technique. *J. Phys. Chem. B* **2006**, *110*, 20263–20267.

(26) Xie, J.; Wang, H.; Duan, M.; Zhang, L. Synthesis and photocatalysis properties of ZnO structures with different morphologies via hydrothermal method. *Appl. Surf. Sci.* **2011**, *257*, 6358–6363.

(27) Zhang, M.; Averseng, F.; Krafft, J.-M.; Borghetti, P.; Costentin, G.; Stankic, S. Controlled Formation of Native Defects in Ultrapure ZnO for the Assignment of Green Emissions to Oxygen Vacancies. *J. Phys. Chem. C* **2020**, *124*, 12696–12704.

(28) Shu, Y.; Duan, X.; Niu, Q.; Xie, R.; Zhang, P.; Pan, Y.; Ma, Z. Mechanochemical Alkali-Metal-Salt-mediated synthesis of ZnO nanocrystals with abundant oxygen Vacancies: An efficient support for Pd-based catalyst. *Chem. Eng. J.* **2021**, *426*, 131757.

(29) Liu, X.; Liu, M. -H.; Luo, Y.-C.; Mou, C.-Y.; Lin, S. D.; Cheng, H.; Chen, J.-M.; Lee, J.-F.; Lin, T.-S. Strong Metal-Support Interactions between Gold Nanoparticles and ZnO Nanorods in CO Oxidation. *J. Am. Chem. Soc.* **2012**, *134*, 10251–10258.

(30) Iwasa, N.; Kudo, S.; Takahashi, H.; Masuda, S.; Takezawa, N. Highly selective supported Pd catalysts for steam reforming of methanol. *Catal. Lett.* **1993**, *19*, 211–216.

(31) Iwasa, N.; Masuda, S.; Ogawa, N.; Takezawa, N. Steam reforming of methanol over Pd/ZnO: Effect of the formation of PdZn alloys upon the reaction. *Appl. Catal. A* **1995**, *125*, 145–157.

(32) Föttinger, K.; van Bokhoven, J. A.; Nachttegaal, M.; Rupprechter, G. Dynamic Structure of a Working Methanol Steam Reforming Catalyst: In Situ Quick-EXAFS on Pd/ZnO Nanoparticles. *J. Phys. Chem. Lett.* **2011**, *2*, 428–433.

- (33) Zhang, H.; Sun, J.; Dagle, V. L.; Halevi, B.; Datye, A. K.; Wang, Y. Influence of ZnO Facets on Pd/ZnO Catalysts for Methanol Steam Reforming. *ACS Catal.* **2014**, *4*, 2379–2386.
- (34) Chen, Y.; Dai, Q.; Zhang, Q.; Huang, Y. Precisely deposited Pd on ZnO (002) facets derived from complex reduction strategy for methanol steam reforming. *Int. J. Hydrogen Energy* **2022**, *47*, 14869–14883.
- (35) Hosseini-Sarvari, M.; Razmi, Z. Palladium Supported on Zinc Oxide Nanoparticles as Efficient Heterogeneous Catalyst for Suzuki-Miyaura and Hiyama Reactions under Normal Laboratory Conditions. *Helv. Chim. Acta* **2015**, *98*, 805–818.
- (36) Hosseini-Sarvari, M.; Bazyar, Z. Visible Light Driven Photocatalytic Cross-Coupling Reactions on Nano Pd/ZnO Photocatalyst at Room-Temperature. *ChemistrySelect* **2018**, *3*, 1898–1907.
- (37) Hosseini-Sarvari, M.; Razmi, Z.; Doroodmand, M. M. Palladium supported on zinc oxide nanoparticles: Synthesis, characterization, and application as heterogeneous catalyst for Mizoroki–Heck and Sonogashira reactions under ligand-free and air atmosphere conditions. *Appl. Catal. A* **2014**, *475*, 477–486.
- (38) Hosseini-Sarvari, M.; Razmi, Z. Direct hydrogenation and one-pot reductive amidation of nitro compounds over Pd/ZnO nanoparticles as a recyclable and heterogeneous catalyst. *Appl. Surf. Sci.* **2015**, *324*, 265–274.
- (39) Hosseini-Sarvari, M.; Razmi, Z. Highly active recyclable heterogeneous Pd/ZnO nanoparticle catalyst: sustainable developments for the C–O and C–N bond cross-coupling reactions of aryl halides under ligand-free conditions. *RSC Adv.* **2014**, *4*, 44105–44116.

(40) Bao, Z.; Yuan, Y.; Leng, C.; Li, L.; Zhao, K.; Sun, Z. One-Pot Synthesis of Noble Metal/Zinc Oxide Composites with Controllable Morphology and High Catalytic Performance. *ACS Appl. Mater. Interfaces* **2017**, *9*, 16417–16425.

(41) Hu, Q.; Liu, X.; Tang, L.; Min, D.; Shi, T.; Zhang, W. Pd–ZnO nanowire arrays as recyclable catalysts for 4–nitrophenol reduction and Suzuki coupling reactions. *RSC Adv.* **2017**, *7*, 7964–7972.

(42) Jeremic, S.; Djokic, L.; Ajdačić, V.; Božinović, N.; Pavlovic, V.; Manojlović, D. D.; Babu, R.; Senthamarai kanna n, R.; Rojas, O.; Opsenica, I. M.; Nikodinovic-Runic, J. Production of bacterial nanocellulose (BNC) and its application as a solid support in transition metal catalysed cross-coupling reaction. *Int. J. Biol. Macromol.* **2019**, *129*, 351–360.

(43) Lin, F.; Chen, Z.; Gong, H.; Wang, X.; Chen, L.; Yu, H. Oxygen Vacancy Induced Strong Metal–Support Interactions on Ni/Ce_{0.8}Zr_{0.2}O₂ Nanorod Catalysts for Promoting Steam Reforming of Toluene: Experimental and Computational Studies. *Langmuir* **2023**, *39*, 4495–4506.

(44) Zhang, C.; Wang, L.; Etim, U. J.; Song, Y.; Gazit, O. M.; Zhong, Z. Oxygen vacancies in Cu/TiO₂ boost strong metal-support interaction and CO₂ hydrogenation to methanol. *J. Catal.* **2022**, *413*, 284–296.

(45) Haque, F.; Chenot, S.; Viñes, F.; Illas, F.; Stankic, S.; Jupille, J. ZnO powders as multi–facet single crystals. *Phys. Chem. Chem. Phys.* **2017**, *19*, 10622–10628.

- (46) Devivaraprasad, R.; Nalajala, N.; Bera, B.; Neergat, M. Electrocatalysis of Oxygen Reduction Reaction on Shape-Controlled Pt and Pd Nanoparticles – Importance of Surface Cleanliness and Reconstruction. *Front. Chem.* **2019**, *7*, 648.
- (47) Stankic, S.; Cortes-Huerto, R.; Crivat, N.; Demaille, D.; Goniakowski, J.; Jupille, J. Equilibrium shapes of supported silver clusters. *Nanoscale* **2013**, *5*, 2448–2453.
- (48) Gedamu, D.; Paulowicz, I.; Kaps, S.; Lupan, O.; Wille, S.; Haidarschin, G.; Mishra, Y. K.; Adelung, R. Rapid Fabrication Technique for Interpenetrated ZnO Nanotetrapod Networks for Fast UV Sensors. *Adv. Mater.* **2013**, *26*, 1541–1550.
- (49) Davey, W. P. Precision Measurements of the Lattice Constants of Twelve Common Metals. *Phys. Rev.* **1925**, *25*, 753–761.
- (50) Ajdačić, V.; Nikolić, A.; Kerner, M.; Wipf, P.; Opsenica, I. M. Reevaluation of the Palladium/Carbon-Catalyzed Decarbonylation of Aliphatic Aldehydes. *Synlett* **2018**, *29*, 1781–1785.
- (51) Balanta, A.; Godard, C.; Claver, C.; Pd nanoparticles for C–C coupling reactions. *Chem. Soc. Rev.* **2011**, *40*, 4973–4985.
- (52) Nemygina, N. A.; Nikoshvili, L. Z.; Tiamina, I. Y.; Bykov, A. V.; Smirnov, I. S.; LaGrange, T.; Kaszkur, Z.; Matveeva, V. G.; Sulman, E. M.; Kiwi-Minsker, L. Au Core–Pd Shell Bimetallic Nanoparticles Immobilized within Hyper-Cross-Linked Polystyrene for Mechanistic Study of Suzuki Cross-Coupling: Homogeneous or Heterogeneous Catalysis?, *Org. Process Res. Dev.* **2018**, *22*, 1606–1613.

(53) Appa, R. M.; Raghavendra, P.; Lakshmidēvi, J.; Naidu, B. R.; Sarma, L. S.; Venkateswarlu, K.; Structure controlled Au@Pd NPs/rGO as robust heterogeneous catalyst for Suzuki coupling in biowaste-derived water extract of pomegranate ash. *Appl. Organomet. Chem.* **2021**, *35*, e6188.

(54) Lakshmidēvi, J.; Vakati, V.; Naidu, B. R.; Raghavender, M.; Krishna Rao, K. S. V.; Venkateswarlu, K. Pd(5%)-KIT-6, Pd(5%)-SBA-15 and Pd(5%)-SBA-16 catalysts in water extract of pomegranate ash: A case study in heterogenization of Suzuki-Miyaura reaction under external base and ligand free conditions. *Sustainable Chem. Pharm.* **2021**, *19*, 100371.